ACS SyntheticBiology

pubs.acs.org/synthbio Research Article

Komagataeibacter Tool Kit (KTK): A Modular Cloning System for Multigene Constructs and Programmed Protein Secretion from Cellulose Producing Bacteria

Vivianne J. Goosens, Kenneth T. Walker, Silvia M. Aragon, Amritpal Singh, Vivek R. Senthivel, Linda Dekker, Joaquin Caro-Astorga, Marianne L. A. Buat, Wenzhe Song, Koon-Yang Lee, and Tom Ellis*

Cite This: *ACS Synth. Biol.* 2021, 10, 3422–3434 Read Online

ACCESS | Metrics & More | Article Recommendations | Supporting Information

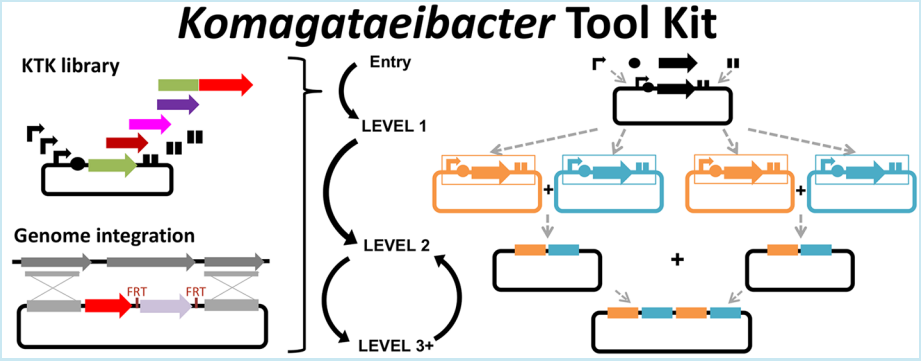

ABSTRACT: Bacteria proficient at producing cellulose are an attractive synthetic biology host for the emerging field of Engineered Living Materials (ELMs). Species from the *Komagataeibacter* genus produce high yields of pure cellulose materials in a short time with minimal resources, and pioneering work has shown that genetic engineering in these strains is possible and can be used to modify the material and its production. To accelerate synthetic biology progress in these bacteria, we introduce here the *Komagataeibacter* tool kit (KTK), a standardized modular cloning system based on Golden Gate DNA assembly that allows DNA parts to be combined to build complex multigene constructs expressed in bacteria from plasmids. Working in *Komagataeibacter rhaeticus*, we describe basic parts for this system, including promoters, fusion tags, and reporter proteins, before showcasing how the assembly system enables more complex designs. Specifically, we use KTK cloning to reformat the *Escherichia coli* curli amyloid fiber system for functional expression in *K. rhaeticus*, and go on to modify it as a system for programming protein secretion from the cellulose producing bacteria. With this toolkit, we aim to accelerate modular synthetic biology in these bacteria, and enable more rapid progress in the emerging ELMs community.

The emerging field of Engineered Living Materials (ELMs) uses synthetic biology to grow and engineer materials with characteristics that are prominent in nature, such as color, self-repair, growth, conductivity, and inherent sensing.[1,2] Being biological, these materials also remain biodegradable and can be grown from sustainable nutrient sources and so have great potential in a circular economy. A significant focus of early ELMs work has been on bacterial biofilms, and in particular, on manipulating proteinaceous amyloid fibers and cellulosic polymers as these lend themselves to a number of ELM-based applications.[1,3]

Bacterial cellulose (BC) is a major component of biofilms and is unique in its purity, synthesis, and network architecture, offering a biocompatible material with superior crystallinity and tensile strength compared to plant cellulose.[4] These physiochemical characteristics of BC has made it valued in the food, beverage, cosmetic, surgical, and biomedical industries and has enormous potential as an ELM.[1,5] Gram-negative acetic acid bacteria (AAB), in particular *Gluconacetobacter* and *Komagataeibacter* species, are prolific producers of BC.

In recent years, many advances have been made in molecular tools for the BC field;[6−10] however, both the general cellulose and the more specific cellulose-based ELM fields could greatly benefit from a Golden Gate (GG) cloning toolkit. Modular

Received: July 28, 2021
Published: November 12, 2021

https://doi.org/10.1021/acssynbio.1c00358
ACS Synth. Biol. 2021, 10, 3422–3434

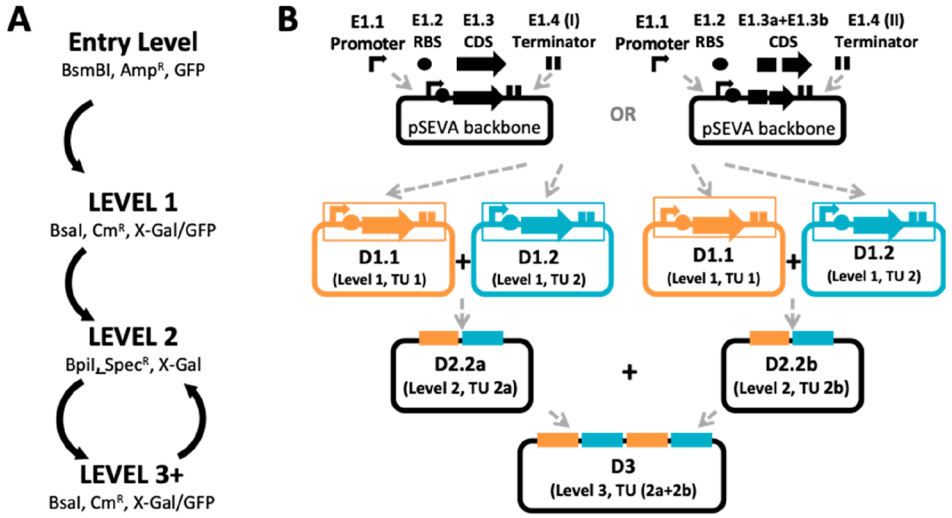

Figure 1. The KTK cloning system. (A) The levels of KTK cloning. Entry-level plasmids are ampicillin resistant (Amp^R), are selected by the absence of GFP, and BsmBI is used for cloning. In Level 1 (and Level 3) cloning plasmids generated using BsaI, resulting in chloramphenicol resistant (Cm^R) plasmids that have lost the X-Gal or GFP marker cassette. BpiI is used in Level 2 cloning and resultant plasmids are spectinomycin resistant and selected for by loss of X-Gal cassette. (B) Schematic of the Entry-level Parts combining with a Level 1 backbone vector to form either a basic TU made up of promoter (E1.1), RBS (E1.2), CDS (E1.3), and terminator (E1.4I) parts or a fusion protein TU made up of promoter (E1.1), RBS (E1.2), fused CDS (E1.3a + E1.3b), and terminator (E1.4II) parts. There are two variations of Level 1 destination vectors and two variation of Level 2 destination vectors. Combined this allows the combination of 4 TUs at the third cloning level. In both Level 1 and Level 2 cloning there are two possible destination vector backbones (D1.1 + D1.2 and D2.2a + D2.2b, respectively). The third cloning level recycles the same destination vectors as in Level 1, facilitating iterative cycles of cloning between the two vector backbones.

GG-based toolkits have revolutionized molecular and synthetic biology in other organisms including in yeasts, mammalian cells, plants, and Gram-positive and Gram-negative bacteria.[11−19] GG cloning is a methodology that exploits the characteristic of Type IIS restriction enzymes (REs) to cut a short distance away from their recognition sites. These enzymes generate unique and orientated DNA overhangs, allowing one to ligate multiple fragments simultaneously in a defined order. As the initial RE site is removed in this process, the ligation is cemented and no recutting of the same site can occur. These cloning systems allow for rapid assembly of DNA constructs from modular genetic parts to build multigene systems, and as such several toolkits with both broad or specific host-ranges have been developed for synthetic biology and are transforming their relevant fields.[20−24]

Recognizing a lack of such a system for BC-producing bacteria, we developed and herein describe the *Komagataeibacter* Tool Kit (KTK): a modular cloning system that caters to *Komagataeibacter* species, the BC biosynthesis field and those developing cellulose-based ELMs. We define our KTK system and the plasmids and part standards associated with it, and then demonstrate its use in *Komagataeibacter rhaeticus*, a transformable native BC producer, in cases using basic parts for gene expression, and then for cases where multigene expression is necessary to achieve new functionality. As a case-study, we used KTK cloning to express *E. coli*'s Curli system, which produces the best-studied bacterial amyloid; a polymeric protein structurally rich in beta-sheets that forms a fiber with exceptional strength, stability, and resistance.[25] Curli has been a focus for many ELM-associated studies,[26−29] and offers promise for making a novel composite with BC in cells that can coproduce both materials. The Curli production system is also representative of a Type VIII secretion system (T8SS) and so its expression offers a tractable solution for protein secretion from BC-producing cells. Expressing this system in *K. rhaeticus* allows us to secrete Curli proteins and enzymes from BC-producing bacteria and demonstrates the power of the KTK system for assembling complex multigene modular assemblies. Further, the KTK system is based on plasmid vectors and selectable markers shown previously to be functional in *K. rhaeticus*, *Komagataeibacter xylinus*, and *Komagataeibacter hansenii*, and therefore, the benefits of the KTK toolkit are likely to be transferable and can be further exploited in these and other high cellulose producing strains.[6,9,30]

RESULTS

The *Komagataeibacter* Toolkit (KTK). The KTK system is an iterative, hierarchical Golden Gate (GG) cloning method best described in levels (Figure 1A). GG cloning takes advantage of Type IIS restriction enzymes (REs). These enzymes cut a short distance away from the recognition site to generate specific overhangs used for orientated ligations. Once these overhangs are joined, the DNA fragment no longer includes the initial RE site, thereby cementing the ligation and prevent recutting (for a detailed guide and illustrations see the Supporting Information). This GG system starts with Entry-level Parts, the basic DNA-encoded components required for gene expression in a single Transcriptional Unit (TU). Entry-level Parts include promoters (E1.1), ribosome-binding site (RBS) sequences (E1.2), coding sequence (CDS) regions (E1.3), and terminators (E1.4) (Figure 1B). The Entry-level Parts are designed to include complementary GG overhangs for oriented ligations, so that when combined in the first level of cloning with a Destination vector backbone they ligate to form a plasmid with a single full Transcription Unit (Figure 1B).

KTK Destination Vectors are based on Standard European Vector Architecture (SEVA) plasmids, and benefit from the advantages of this powerful modular set.[31] The main destination vectors are adapted from the pSEVA331 and

https://doi.org/10.1021/acssynbio.1c00358
ACS Synth. Biol. 2021, 10, 3422−3434

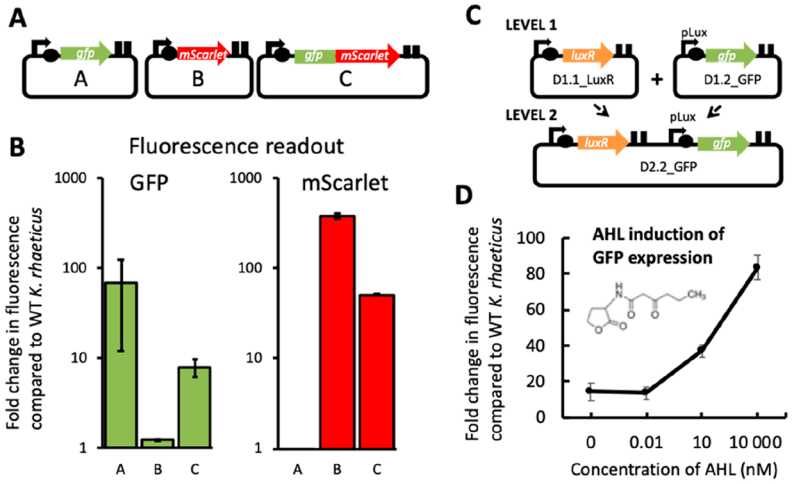

Figure 2. Validation of KTK cloning for basic TU and fused TU constructs (Level 1) and a multigene cassette (Level 2). (A) Design of the assembled fluorescent protein expressing constructs used to validate KTK Level 1 cloning. All promoters used are J23104. (B) Fluorescence per cell measured by flow cytometry of *K. rhaeticus* strains expressing GFP, mScarlet or a fused GFP-mScarlet protein. Values normalized to untransformed *K. rhaeticus* with GFP fluorescence shown in green and mScarlet in red. Error bars represent SD of three replicates. (C) Cloning schematic showing the use of different Destination vectors to enable Level 1 to Level 2 cloning. Level 1 assembly results in a LuxR-expressing TU (with J23104 promoter), and a TU with pLux promoter and GFP. Level 2 cloning brings these TUs together to give an AHL-inducible GFP expressing plasmid. (D) *K. rhaeticus* strains with the plasmid constructed in (c) were exposed to a range of exogenous AHL concentrations in liquid growth phase and mean GFP fluorescence per cell was measured by flow cytometry. Error bars show standard deviation, $n = 3$.

pSEVA431 plasmids, which have a pBBR1 replication origin and encode Chloramphenicol and Spectinomycin resistance markers, respectively. Previous studies have shown that these plasmid vectors actively express proteins in *K. hansenii*, *K. xylinus*, and *K. rhaeticus*. Transformation efficiencies in *K. hansenii*, *K. xylinus* are significantly lower than those seen in *K. rhaeticus*,[6−10,30] therefore for the purpose of creating and validating this toolkit we focused on *K. rhaeticus*. In the KTK system, the multiple cloning site (MCS) regions of pSEVA331 and pSEVA431 plasmids have been modified to encode Golden Gate cloning sequences. A further possibility when constructing a TU with KTK is to create a fusion protein in the CDS position (E1.3). The system allows this by ligating C- and N-terminal domain CDS parts (E1.3a and E1.3b) (Figure 1B). The basic KTK system includes a library of useful Entry-level Parts (promoters, RBS, terminators, and useful C- and N-terminal CDS domains, e.g., GFP, His-tag and signal peptides) as well as sequences that can be used as "spacers" that are useful at subsequent cloning levels. All plasmid construction is designed to be done using *E. coli* cloning strains, before completed plasmids are then transformed into competent *K. rhaeticus* for testing.

For simple constitutive expression of a protein, constructing a TU via a single round of cloning (level one) is sufficient. However, for multifaceted genetic constructs, such as inducible expression cassettes or multipart TUs, the KTK adds further cloning levels that enable versatile construction. The backbone vectors for each cloning level have an alternating arrangement of flanking Type IIS RE sites (for BsaI and BpiI). These in turn generate specific overhangs that are used for the next level of cloning (illustrated and detailed in Supporting Information). The nature of Type IIS RE cloning means that one of set of RE sites are removed during the ligation reaction and the second set then becomes available for the next level of assembly. Furthermore, the KTK system provides two Backbone vectors for each cloning level, each with slight variation in overhangs to allow for the parallel insertion of different ligated DNA parts and TU assemblies. These can then be joined in the next level of ligation, thereby facilitating multiple cycles with multipart constructs (Figure 1B).

Validating KTK Golden Gate Cloning. To validate Level 1 Golden Gate assembly with KTK, plasmids were constructed to express fluorescent proteins from encoded TUs. Entry-level Parts were first prepared, including the well-characterized constitutive promoter J23104 (E1.1),[7,8] a standard RBS (E1.2), a terminator (E1.4), and CDS parts (E1.3) encoding two fluorescent proteins, superfolder Green Fluorescent Protein (sfGFP) and mScarlet Red Fluorescent Protein (RFP). These two CDS parts were also cloned as N-terminal (E1.3a) and C-terminal (E1.3b) CDS parts to also allow assembly of a TU expressing sfGFP-mScarlet fusion protein (Figure 2A). Assembly of basic and fusion TU constructs was done using the KTK system with cloning steps in *E. coli*. The three constructs were then transformed into *K. rhaeticus* competent cells, and selected transformant colonies were then cultured in liquid growth media in the presence of purified cellulase (to prevent material formation) and measured for green and red fluorescence by flow cytometry (Figure 2B). The fluorescence intensity per cell compared to untransformed cells showed strong expression of both reporter proteins in basic TU form, and expression with reduced strength when constructed as a fusion protein.

Next, a multigene Level 2 construct was designed to yield a plasmid encoding externally inducible GFP expression. Previous *K. rhaeticus* studies have taken advantage of the Vibrio Lux quorum sensing system for external gene expression induction.[7−9] In the Lux system a regulator protein (LuxR) binds and induces expression of the gene coupled the pLux promoter when LuxR is bound to an acyl homoserine lactone (AHL). In the design chosen here, LuxR-AHL triggers expression of GFP. This two-gene construct was assembled by KTK cloning from Entry-level Parts. Unlike in cloning of a single TU, choice of Level 1 Destination vectors is important when going to Level 2. This is due to the overhang sequences

https://doi.org/10.1021/acssynbio.1c00358
ACS Synth. Biol. 2021, 10, 3422−3434

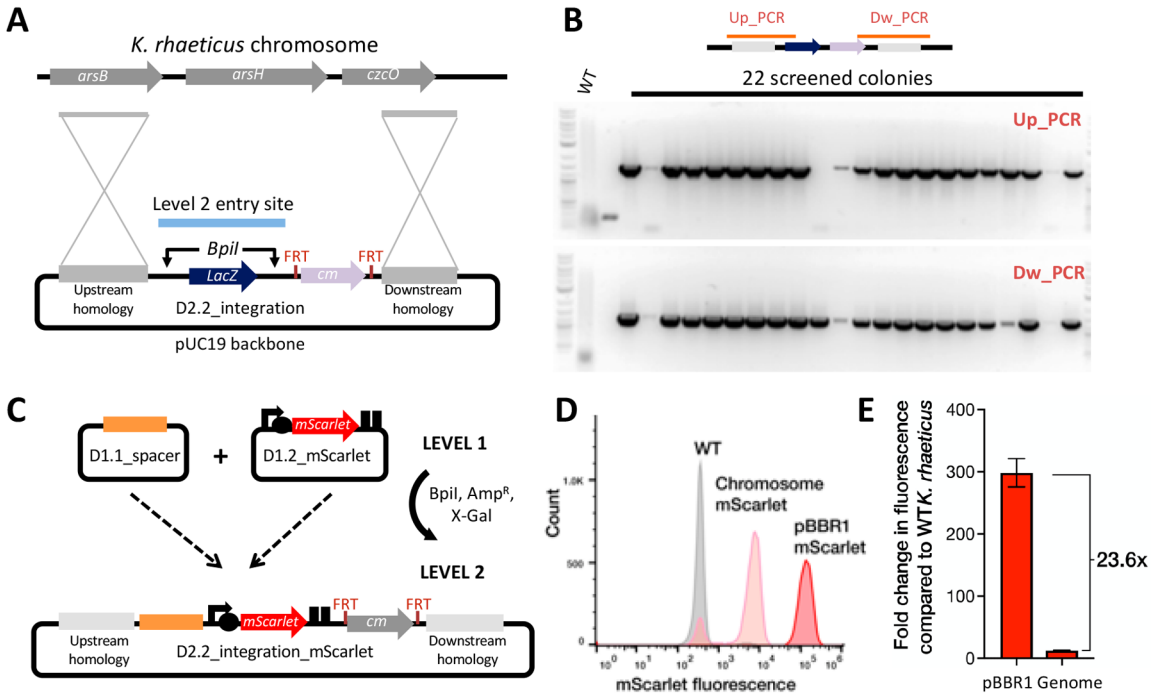

Figure 3. A KTK system for genome integration. (A) The D2.2_integration plasmid is based on the ampicillin resistant pUC19 backbone with homologous recombination into the *K. rhaeticus* chromosome guided by two regions of homology (upstream: 1000 bp, downstream: 921 bp) to the arsenic resistance operon. Between these regions of homology is a KTK Level 2 entry site, with a LacZ dropout cassette, and a FRT-site-flanked chloramphenicol resistance gene for selection in *K. rhaeticus*. (B) Confirmatory PCR analysis of 22 screened colonies. (C) Construction of a KTK Level 2 plasmid for integration into *K. rhaeticus*. D1.1_spacer and D1.2_mScarlet (using J23104 promoter) were built into the D2.2_intergration backbone by standard KTK Level 2 assembly, with the single alteration of antibiotic selection on ampicillin instead of spectinomycin. (D) Representative flow cytometry distributions of *K. rhaeticus* strains expressing the same mScarlet expression construct from the chromosome (pink) and pBBR1 plasmid (red), compared to no expression in wildtype cells (gray). (E) RFP signal from mScarlet expression when on pBBR1 plasmid vs genome-integrated, as determined by flow cytometry. Red fluorescence is measured as fold increase over wildtype reading and is an the average of biological triplicates. The per cell copy number of pBBR1 plasmid (×23.6) is estimated from the difference between fluorescence of the two average values.

generated by digestion that are designed into the KTK vectors. Each overhang is unique and allows for a sequential combination of fragments. When combining a simple transcriptional unit in Level 1, this sequence follows a standard genetic logic (promoter-RBS-CDS-terminator). However, when combining plasmids from Level 1 into Level 2 Destination vectors one needs to take note of the vector backbone, as each backbone's unique overhangs have a direct influence on the downstream arrangement when combining multiple TUs. This is visualized in Figure 1B and detailed in the KTK guide and illustrations provided in the Supporting Information.

A TU constitutively expressing LuxR was assembled into a D1.1 vector, while the TU expressing sfGFP from the pLux promoter was assembled into a D1.2 vector (Figure 2C). The multigene Level 2 construct was then assembled from Level 1 constructs and transformed into *K. rhaeticus*. This construct worked as expected showing induction of GFP expression in the presence of increasing AHL concentrations (Figure 2D).

Genomic Integration of KTK Constructs. In addition to plasmid-based expression, it is regularly desirable to have integration of constructs into the host cell genome. To enable this feature as part of the KTK system, we modified a pUC19-based *E. coli* plasmid that does not replicate in *Komagataeibacter* so that the DNA cargo held in this vector had two regions of homology to the chromosome flanking a chloramphenicol selectable marker gene (Figure 3A). Transformation of high concentrations of this plasmid, along with stringent antibiotic selection were expected to lead to integration of the DNA between the homology sequences at the desired chromosomal locus. To test this we targeted the genome locus for arsenic resistance, designing 1 kb homology sequences that match regions of the *arsB* and *czcO* genes that flank the *arsH* gene. These sequences were placed in the pUC19 vector either side of a Level 2 cloning entry site (lacZ gene flanked by BpiI sites) and the chloramphenicol selectable marker gene, which itself was flanked by FRT sites that are recognized by the Flp flippase. This formed the D2.2_integration vector, a general KTK-compatible vector for genomic integration in place of *arsH*. Transformation of this plasmid into competent *K. rhaeticus* cells proved highly efficient for targeted genome integration, with 18 out of 22 selected colonies showing correct integration at the *arsH* locus when tested by PCR analysis (Figure 3B).

To demonstrate using this as part of the KTK system, we performed an assembly of two Level 1 constructs, a spacer module and a TU for constitutive mScarlet RFP expression, into the D2.2_integration plasmid (Figure 3C) and used the resulting construct to generate a *K. rhaeticus* strain with single-copy chromosomal RFP expression (Figure 3D). Using flow cytometry to compare the red fluorescence per cell of this strain to strains where the same mScarlet TU is maintained on a typical KTK plasmid (with pBBR1 ori) gave us a quantitative inference of plasmid copy number (Figure 3E). This revealed

https://doi.org/10.1021/acssynbio.1c00358
ACS Synth. Biol. 2021, 10, 3422−3434

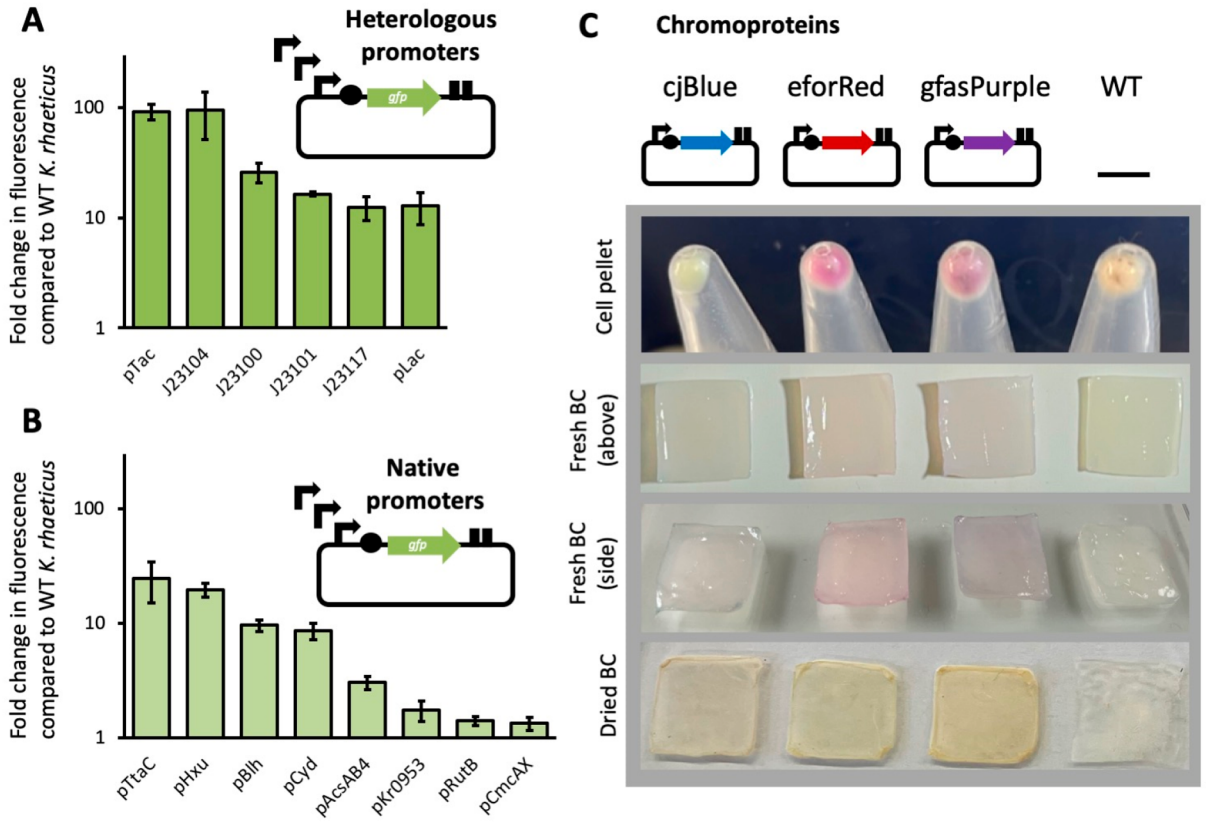

Figure 4. Characterization of promoters for the KTK parts library. (A) Fluorescence per cell measured by flow cytometry of *K. rhaeticus* strains expressing GFP in a standard single TU from 6 different heterologous promoters. (B) Fluorescence per cell measured by flow cytometry of *K. rhaeticus* strains expressing GFP in a standard single TU from 8 native promoters. Values in the plots are normalized to untransformed *K. rhaeticus*. Error bars represent SD of three replicates. (C) Cell pellets (top row), fresh BC pellicles (middle two rows), and air-dried BC pellicles (bottom) from cells transformed with plasmids expressing 3 representative chromoprotein reporters.

for the first time that the plasmids used here and in our past studies in *K. rhaeticus* are present at an average copy number of around 23 copies per cell. This estimate was further confirmed by qPCR analysis of the DNA in these strains.

The D2.2 integration vector described here targets the *ars* locus due to the selected homology regions; however, due to the design these regions could be easily exchanged (e.g., by Gibson assembly) for alternative 1 kb homology regions targeting insertion into other loci, both to deliver new constructs into the genome, and also to delete or replace genomic DNA targets. The inclusion of FRT sites also opens up the future option of removal of the integrated selectable marker gene by transient expression of the FRT flippase enzyme.[32]

Expanding and Characterizing the KTK Parts Library. The utility of GG-based cloning toolkits are dependent on the size, characterization and availability of its parts. To populate the KTK system we prepared a library of shareable Entry-level Parts as well as useful destination-level plasmids (Table S1). This library includes a panel of promoters, RBS sequences, terminators, and basic CDS parts (selection cassettes, fluorescent proteins) as well as spacer sequences that enable more complex assembly steps. Our basic library will be made available to researchers and is intended to become a resource for the wider community.

As tuning gene expression is a key goal in engineering cells, we characterized a panel of promoters including heterologous promoters and promoters native to *K. rhaeticus*, with the latter identified from genes and operons known to express from the strain genome. KTK enabled straightforward and quick assembly of modular constructs expressing sfGFP in basic TUs, each with a different promoter. These promoters were then characterized for expression strength in liquid growth phase using flow cytometry quantification of green fluorescence. J23104 and pTac promoters were the strongest heterologous promoters (Figure 4A), while the native promoters pTtcA and pHxu were the strongest of the ones taken from the genome sequence (Figure 4B). The individual strengths of the heterologous promoters in KTK format correlate well to their strengths measured in past work in this strain in different DNA formats.[7,9]

We further sought to add reporter proteins visible to the naked eye that can be expressed within cellulose materials. To this end, we cloned 3 chromoproteins previously characterized in *E. coli*[33] that are visibly blue (cjBlue), red (eforRed), and purple (gfasPurple). When expressed in *K. rhaeticus* as a Level 1 construct with J23104 promoter, each chromoprotein was able to change the color of the bacterial cell pellet (Figure 4C), although cjBlue gave a more greenish hue than expected. The resulting bacterial cellulose pellicles grown from these strains showed visible coloration of the material, with the red and purple colors being particularly striking. However, on dehydration of the cellulose, pigmentation was lost, although

https://doi.org/10.1021/acssynbio.1c00358
ACS Synth. Biol. 2021, 10, 3422−3434

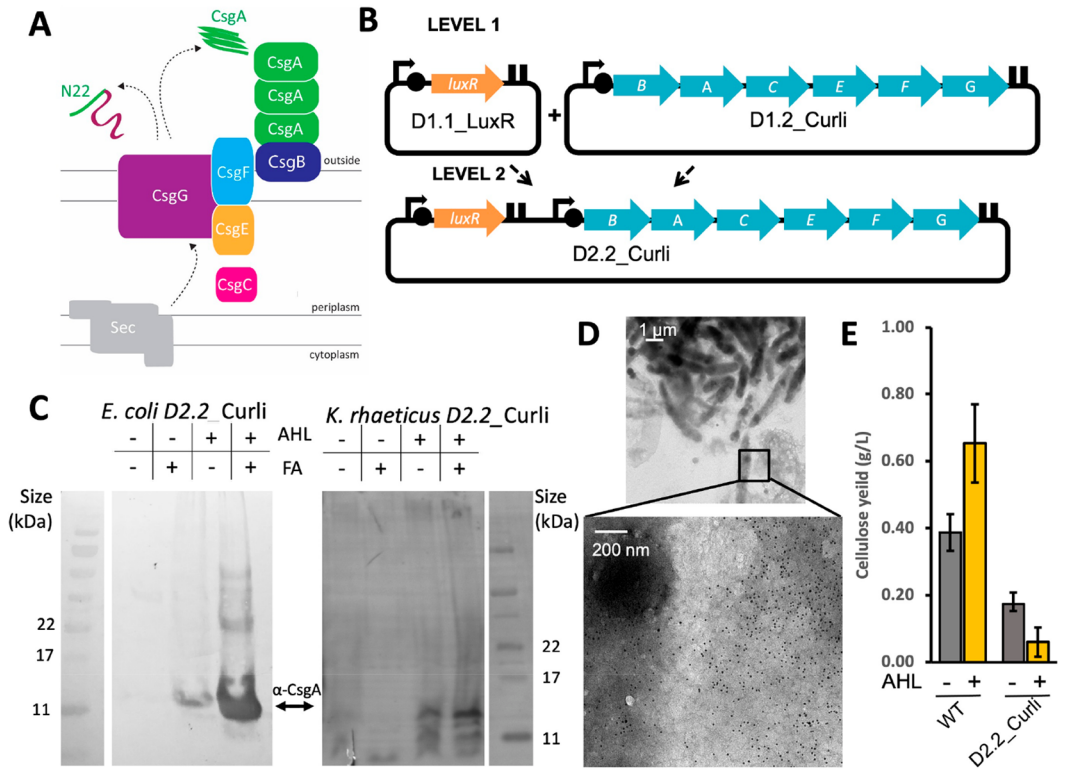

Figure 5. Expressing an inducible Curli system in *K. rhaeticus*. (A) Schematic of the *E. coli* Curli system where amyloid fibers are assembled composed of polymers of CsgA, nucleated to the cell surface via CsgB. These proteins are chaperoned (CsgC) and transferred over the outer membrane via a specialized Type VIII secretion (T8S) system (CsgE, CsgF, CsgG). All proteins are secreted into the periplasm via the Sec system; however, the N22 region of CsgA (shown in green) is essential for directing the protein through the CsgG pore in the outer membrane. (B) Cloning schematic illustrating the KTK assembly of the AHL-inducible, Curli-expressing D2.2_Curli plasmid from two Level 1 plasmids. (C) Western blot of protein extractions from *E. coli* and *K. rhaeticus* cultures transformed with the D2.2_Curli plasmids. Cultures were grown with or without AHL inducer and obtained extracts were treated with or without Formic Acid (FA) to denature Curli proteins. Polyclonal anti-CsgA antibody was used for detection and the CsgA band is indicated with an arrow. (D) Transmission electron microscopy visualization of gold particle-stained Curli proteins outside of a D2.2_Curli expressing *K. rhaeticus* (inset). Black dots in the high magnification image are gold nanoparticles bound to the Curli protein via α-CsgA rabbit antibody and 10 nm antirabbit IgG-Gold coupled antibody. (E) Mean dry pellicle weight for wildtype (WT) *K. rhaeticus* and *K. rhaeticus* with D2.2_Curli, with (+) and without (−) the addition of AHL inducer; error bars show standard deviation, $n = 3$.

the final material was still notably a different shade to cellulose made from unmodified cells (Figure 4C, Figure S1).

The basic KTK parts library contains several reporter proteins, terminators, RBS sequences, and constitutive promoters, as well as the AHL-inducible promoter (Figure 2) and will be shared as a distributable collection of the most relevant plasmids. We anticipate expanding this in the near future to include more inducible expression systems and have already designed a dedicated KTK construct to enable CRISPR-based gene regulation (Figure S2).

KTK Construction of an Inducible Curli System. For a case-study application of the KTK system, we next designed and constructed a multigene assembly to express and extrude Curli amyloid fibers from *K. rhaeticus*. In *E. coli*, Curli fibers are polymerized on the outer surface of the cell from monomers of the CsgA protein, with this facilitated by five other Curli proteins that act to chaperone (CsgC) and nucleate (CsgB) fiber formation, and form a Curli-specific type VIII secretion system (T8SS) (CsgE, CsgF, CsgG) through the outer membrane[25,34] (Figure 5A). In *E. coli* these genes are encoded on two divergent operons; however, a number of landmark ELM studies have elegantly functionalized Curli by rearranging these genes into an easier-to-engineer synthetic linear operon.[35] The linear operon format enables researchers to more readily modify Curli through C-terminal CsgA fusions (small peptides or whole proteins) or by exploiting the signal peptide (the first 22 amino acids of CsgA) to secrete heterologous proteins through the Curli T8SS.[27−29,36−42]

To port the *E. coli* Curli system into BC-producing bacteria, we chose to maintain the linear operon format successfully employed in past ELMs work. The region encoding the 6 genes from the synthetic *E. coli* operon was therefore cloned into a KTK entry-level vector as if it was a single CDS (E1.3) part (Figure 5B). This was then assembled into a Level 1 Curli-containing plasmid (D1.2_Curli), with the AHL-inducible pLux promoter (E1.1), a well-characterized terminator (E1.4I) and an RBS (E1.2) part, selected by the RBS Calculator[43] to give a similar predicted strength for CsgB translation as that seen in the native *E. coli* system. D1.2_Curli was then assembled with a Level 1 LuxR-expressing plasmid (D1.1_LuxR) to create the multigene Level 2 plasmid construct giving AHL-inducible Curli expression (D2.2_Curli). In this design LuxR is expressed by a medium strength promoter (pLac) to reduce any potential burden.

As KTK constructs are compatible in *E. coli*, assays for plasmid function can be performed in *K. rhaeticus* and *E. coli* in

https://doi.org/10.1021/acssynbio.1c00358
ACS Synth. Biol. 2021, 10, 3422−3434

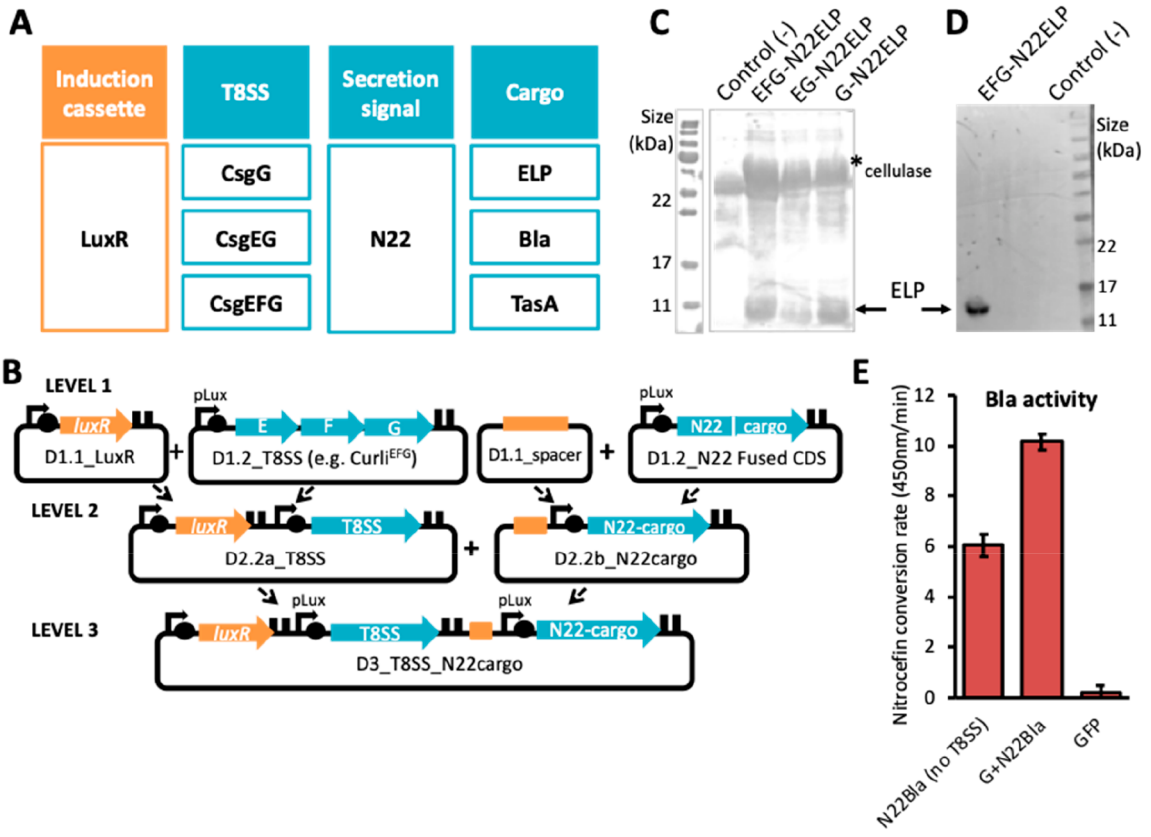

Figure 6. Using a T8SS module to secrete heterologous cargo proteins. (A) Modular components of the KTK-based T8SS constructs. The first module (orange) represents the induction cassette (LuxR) for controlling gene expression, further modules (teal) are 3 versions of the T8SS (CsgG, CsgEG, and CsgEFG), the secretion signal (N22), and the heterologous cargo proteins (ELP, Bla and TasA). (B) Cloning schematic to generate an AHL-inducible modularized T8SS for heterologous protein secretion using the KTK system. Four Level 1 constructs are made: an induction cassette construct (D1.1), the secretion system construct (D1.2), a spacer construct (D1.1), and constructs that fuse the secretion signal (N22 sequence) to the cargo protein (D1.2). These are combined in pairs to Level 2 into the D2.2a and D2.2b vectors. A final assembly creates the Level 3 construct, D3_T8SS_N22cargo, which contains both an inducible secretion target and secretion system. (C,D) SDS-PAGE (C) and Western Blot (D) of samples extracted from culture supernatants from AHL-induced *K. rhaeticus* strains expressing a T8SS module (CsgEFG, CsgEG and CsgG) and N22-ELP-his. To aid liquid phase growth and remove cellulose material, exogenous purified cellulase was added to the cultures and is clearly visible in the SDS-PAGE protein gel. (E) Nitrocefin assay measuring the Beta-lactamase (Bla) activity of supernatant harvested from an induced *K. rhaeticus* strain designed to express CsgG and N22-Bla. An inducible strain expressing GFP (D2.2_GFP) was used as a negative control in this experiment. Error bars represent SD of three replicates.

parallel. To test for expression and production of CsgA from the D2.2_Curli construct, we first used Western blot analysis. As amyloid fibers are resistant to heat and detergents, formic acid (FA) treatment is required for depolymerization prior to SDS-PAGE separation of CsgA and so can be used to identify if the CsgA is polymerized or just in monomeric form. Protein extracts taken from uninduced or AHL-induced *K. rhaeticus* and *E. coli* were separated and stained (Figure 5C) for monomeric CsgA (visible band with no FA treatment) and polymeric CsgA (visible band only seen with FA treatment), confirming that the D2.2_Curli construct produced CsgA and polymerized it into Curli fibers in both *K. rhaeticus* and *E. coli*.

Transmission electron microscopy (TEM) was next performed to visualize Curli fiber production from transformed *K. rhaeticus*. As control, TEM analysis of AHL-induced *E. coli* showed clear filamentous Curli structures (Figure S3A) confirming the plasmid function in this bacterium. Direct visualization was more challenging with *K. rhaeticus* due to cellulose fibers being present in large amounts, even after 20% (w/v) cellulase treatment (Figure S3B). Therefore, to distinguished Curli from cellulose, TEM samples were treated with CsgA-polyclonal antibody and immunogold-labeled. Gold nanoparticle staining was evident in a tangle of fibers outside the *K. rhaeticus* cell, demonstrating that the plasmid is functional in the cellulose-producing bacterium (Figure 5D and Figure S3B). Heterologous expression of proteins is known to be stressful to bacteria and cause burden,[44] therefore, the effect of expression of the Curli membrane protein system on cellulose production was also investigated by growing pellicles from this strain and measuring their weight. This revealed a significant negative effect on cellulose production when cells express the Curli system (Figure 5E). Much thinner pellicles were observed than those of cells engineered to express transcription factors, fluorescent proteins and chromoproteins (for example in Figure 4).

Pellicles were left to grow for a extended period of time, and the effect of induced coproduction of Curli on the material properties of grown bacterial cellulose was then investigated to see if this cellulose-amyloid composite had improved mechanical properties compared to cellulose alone. Strength tests were performed on pellicles grown from AHL-induced *K. rhaeticus* with the D2.2_Curli construct (Figure S3C).

https://doi.org/10.1021/acssynbio.1c00358
ACS Synth. Biol. 2021, 10, 3422−3434

Pellicles grown from cells containing the D2.2_GFP construct were used as a comparable control and controlled for by material thickness. No significant difference in strength was observed between the control and Curli-positive pellicles, likely due to a very low relative abundance of Curli compared to cellulose in the final material.

Programming Protein Secretion via the Type VIII Secretion System. For an example of a Level 3 KTK multigene assembly, we next constructed a plasmid that exploits the Curli-specific T8SS system for heterologous protein secretion (Figure 6A). Previous studies have shown that the first 22 amino acids (N22) of CsgA are enough to target small heterologous proteins for secretion via T8SS.[38,39] To make use of this we split the Curli operon into modules, with the 3 genes encoding the T8SS (CsgE, CsgF, CsgG) as a key part and the N22 signal used as a tag to be fused to proteins for secretion (Figure 6A).

A panel of three T8SS modules were cloned into KTK as CDS parts; the minimal T8SS (just the secretion pore CsgG), CsgG plus the CsgE "adapter protein" (CsgGE), and both of these proteins plus secretion chaperon CsgF (CsgEFG).[45,46] These were assembled to Level 2 with a LuxR TU, so that expression of these T8SS modules was AHL-dependent (Figure 6B). In parallel, a small panel of heterologous cargo targets were prepared using the 2-part CDS fusion approach of KTK to bring together the N-terminal N22 region of CsgA (E1.3a part) with C-terminal CDS parts (E1.3b) encoding three targets: a 98 amino acid elastin-like protein (ELP), the enzyme Beta-lactamase (Bla), and the Gram-positive amyloid protein TasA (Figure 6A,B). ELPs are small unstructured versatile proteins that are highly hydrophobic and an attractive ELM component,[47] Beta-lactamase is a classic enzyme easily detected by the colorimetric nitrocefin assay,[48] and TasA is an amyloid protein from *B. subtilis* that could be an alternative to Curli.[49]

The 3 heterologous cargo targets were assembled into a Level 1 TU construct with the pLux promoter, before then being each combined into a Level 2 construct with a short spacer part (D1.2_Spacer, 23 bp) designed to assist cloning of an odd number of TUs in a multigene assembly (Figure 6B). With all modules now in place in Level 2 plasmids, a combinatorial set of nine possible Level 3 constructs could be assembled with the 3 different T8SS versions and 3 cargo proteins (Figure 6A).

To test the function of these constructs, we again performed experiments in parallel in*E. coli* and *K. rhaeticus* transformed with constructs, culturing with AHL induction and then harvesting in mid log growth phase and separating supernatant and cell fractions. We first assessed ELP expression and secretion, using SDS-PAGE of both *K. rhaeticus* (Figure 6C) and *E. coli* (Figure S4A) samples to confirm the presence of processed and secreted ELP when any one of three T8SS versions were present. As ELP proteins are difficult to transfer by Western Blot due to their hydrophobic nature, the constructs were designed to include a C-terminal his-tag. This enabled us to identify that the 10 kDa protein observed in the secreted fraction was indeed ELP-his when either *K. rhaeticus* (Figure 6D) or *E. coli* (Figure S4B) were expressing the CsgEFG T8SS constructs. Similar experiments with the TasA cargo were not as successful, only showing a small amount of TasA in cell fractions of *E. coli* (Figure S4C), suggesting that TasA cannot use the Curli T8SS for export.

Finally, we assessed enzyme secretion from the beta-lactamase (Bla) encoding Level 3 constructs, as before testing in both *E. coli* and *K. rhaeticus*. Beta-lactamase converts nitrocefin from a yellow to red color, which is quantifiable by spectroscopy at 450 nm and initial *E. coli* data showed that in the presence of either T8SS version, Bla enzymatic activity in the supernatant was higher than when no T8SS was present (Figure S4D). In this case the minimal T8SS (CsgG) gave the highest values, so the Level 3 construct expressing this with N22-Blac was then assessed in *K. rhaeticus*. Supernatant from an AHL-induced culture of these bacteria showed beta-lactamase activity nearly 2-fold higher than when no T8SS is expressed in the cells (Figure 6D). Altogether the results with ELP and Bla cargos show that the modular T8SS system generated here for the KTK system can be used to program protein secretion from *K. rhaeticus*. However, as shown in Figure 4E, the expression of this heterologous T8SS does impose a burden on the bacteria that reduces their cellulose productivity. While this burden is particularly strong when curli fibers are secreted, it is not as extreme with other cargo proteins, such as ELPs (Figure S5). Further work is needed to understand the optimal T8SS version, its ideal expression level, and what design considerations are needed for protein cargo, their secretion, and how to reduce the burden of this system.

CONCLUSION

Through a standardized hierarchical Golden Gate DNA assembly approach, the KTK system allows modular construction of single genes and multigene systems for cellulose-producing *Komagataeibacter*, including the option of single-copy genome integration. We here validated this toolkit using fluorescent protein and chromoprotein constructs, before applying it to the modular construction of plasmids that enable inducible production of Curli fibers by *K. rhaeticus* and heterologous protein secretion by this strain. These examples demonstrate the power of the combinatorial and modular toolkit system.

We provide a selection of basic parts along with the KTK system for tuning, controlling and measuring gene expression. Using promoters and RBS parts of different strength is a powerful way to optimize gene function in bacteria. Most of the experimental results shown here were done without any optimization of expression of assembled genes. Design-led or combinatorial approaches choosing from promoter and RBS libraries are likely to be able to improve on the results seen here for the various demonstrations, for example in helping to make an updated GFP-RFP fusion construct (Figure 2C) that maintains equivalent fluorescence to constructs expressing only one of the two proteins.

To demonstrate how multigene assembly with the KTK system can advance engineered living materials, we imported the well-studied *E. coli* Curli fiber production system into KTK and used it to engineer a construct that instructs *K. rhaeticus to* cosecrete Curli fibers alongside cellulose as material is produced. Although KTK-based cloning was successful in enabling the production of amyloid Curli outside the cell, this did not result in any marked change in material properties for the cellulose-Curli composite pellicle. This is likely due to relatively very low production of protein compared to cellulose from these bacteria, or could be related to Curli fiber formation being impaired chemically by the low pH of *K. rhaeticus* cultures, or physically by the large amounts of cellulose being extruded from the cell surface. In future work, Curli production

https://doi.org/10.1021/acssynbio.1c00358
ACS Synth. Biol. 2021, 10, 3422−3434

could be improved by increasing gene expression with different promoter/RBS parts and by using alternative gene arrangements, e.g., by using strong promoters and a two-module design.[50−52]

The potential of the Curli system was further exploited here by taking advantage of its Type VII secretion system (T8SS) to export heterologous cargo proteins. An N-terminal fused N22 region from CsgA enabled secretion of a small unstructured ELP proteins when expressed in cells coexpressing the CsgEFG T8SS. The tag also gave promising results with Bla for the secretion of active globular enzymes from *K. rhaeticus* strains expressing CsgG. This offers the first described route to getting enzymes expressed in BC-producing bacteria to be secreted extracellularly, opening up the possibility of having cellulose-binding or cellulose-modifying enzymes coproduced as the cellulose material is grown. However, the burden of this system, the relatively low levels of protein and enzyme activity observed, and the failure to secrete TasA suggests that achieving high-level programmed secretion of a desired target protein will more often than not be a challenge and will likely to require significant optimization.

We hope that many people will use and contribute to the KTK system in the future, to add more genetic parts that enable rapid optimization of constructs in BC-producing bacteria. The parts and toolkit described here and in the Supporting Information currently remain untested in other BC-producing strains, but we are optimistic that they will work well in all *Komagataeibacter* and other Acetobacter species. Indeed modular DNA parts developed previously by us and others for *K. rhaeticus* have been shown to be functional in *Komagataeibacter xylinus* and *Komagataeibacter hansenii*.[6−10,30] Parts from these past publications, including promoters, RBS sequences, and CRISPR-derived gene regulation tools, can presumably be reformatted to work within our KTK system. We look forward to many interesting and innovative genetic parts being added to this toolkit as the growing community in synthetic biology and material sciences begin to produce BC-based ELMs with new functionalities and diverse and exciting properties.

MATERIALS AND METHODS

Strains and Culture Conditions. The *E. coli* Turbo (NEB) was used throughout this study. Cultures were grown at 37 °C in shaking liquid Lysogeny Broth (LB) (10 g/L Tryptone, 5 g/L Yeast Extract, 5 g/L NaCl) or on LB agar (1% agar), and when appropriate supplemented with ampicillin (100 μg/mL), chloramphenicol (34 μg/mL), or spectinomycin (100 μg/mL). Transformation was done using chemically competent cells.

K. rhaeticus iGEM cultures were grown at 30 °C in liquid Hestrin−Schramm media (HS) (2% glucose, 10 g/L yeast extract, 10 g/L peptone, 2.7 g/L Na_2HPO_4 and 1.3 g/L citric acid, pH 5.6−5.8) or on HS agar plates (1.5% agar). When growing shaking cultures the media was supplemented with 2% cellulase (Sigma Aldrich, C2730) and, when appropriate, supplemented with chloramphenicol (34 μg/mL) or spectinomycin (100 μg/mL). Electroporation of *K. rhaeticus* strains was performed as described previously.[7] For genome integration, electroporation of *K. rhaeticus* strains was conducted using 2 μg of integration vector DNA. Transformants were screened on 10× chloramphenicol (340 μg/mL) or 5× spectinomycin HS plates (500 μg/mL).

When preparing pellicles for strength tests, *K. rhaeticus* strains were first grown to high density in liquid in the presence of 1× antibiotic. This was then washed twice with HS media, resuspended in fresh cellulose-free HS media to a density of 0.5 OD_{600}. This density was also used as standard for pellicle inoculums. Pellicles were grown stationary at 30 °C in fresh cellulase free HS media (75−100 mL), supplemented with antibiotic, and when appropriate 50 mM AHL. Thick pellicles were observed and harvested after 2−4 weeks.

For measuring cellulose productivity, *K. rhaeticus* strains were grown in 5 mL HS media in a deep 24 well grid plate, incubating at 30 °C in static conditions for 5 days to allow for pellicle growth. Pellicles were then removed from the media and washed in dH_2O for 2 h shaking at 30 °C, with water being replaced after 1 h of incubation, in order to remove media from within the pellicle. Pellicles were then dried in a 60 °C incubator for 2 h to allow pellicles to dry completely before being weighed to determine dry weights.

Molecular Techniques, Primers, and Plasmids. Modular DNA parts and plasmids used and constructed in this study are listed in Supplementary Tables S1 and S2. Standard PCR or primer joining was used to generate the DNA fragments for the Entry-level Parts. PCR was performed by standard protocol using a high-fidelity polymerase as per manufacturer's instructions. Primers are designed to include BsmBI and BsaI required for cloning as detailed in sequences shown in Supplementary Table G1 and Figure G1. If Entry-level Parts were small (<60 bp), instead of a PCR reaction, a primer joining protocol was used. Each primer would cover the target sequence and including the overhang and RE sites detailed in Supplementary Table G1 and Figure G1. In order to allow primers to anneal together a sequence of overlap of at least 15 bp is required. Oligos (100 μM) are separately phosphorylated with T4 PNK (NEB) before combined and heated to 96 °C for 6 min. Samples are annealed by ramping down to 0.1 °C per second until 23 °C. Ten μL of the mixture was used to clone into the Entry-level Backbone vectors.

Golden Gate (GG) assembly followed standard GG protocols published.[16] Briefly T4 DNA Ligase (Promega, C1263), T4 ligase (0.5 μL; NEB, M0202), Type IIs RE (0.5 μL, NEB), vector backbone and inserts were combined to make 10 μL. For optimum results a ratio of insert to backbone of 1:2 was used, i.e., 50 fmol/μL per insert to 25 fmol/μL of backbone. Thermocyclers were used for assembly with 25 cycles of digestion at 42 °C (2 min) and ligation (16 °C, 5 min), before two heat inactivation steps at 60 °C (10 min) and 80 °C (10 min). After which DNA was be transformed as per standard protocols and plated on prepared selectable plates.

Although GG was used primarily, Gibson cloning was required to adapt more complex Entry-level Parts, specifically the removal of BsaI restriction enzyme site from the CsgB gene in the synthetic Curli operon, and when building the CsgE-CsgG operon. All entry-level vectors were sequenced and subsequent plasmids were confirmed with overlapping PCR to ensure all the fragments were present and had combined correctly.

Efficient extraction of genomic DNA from *K. rhaeticus* was conducted using the GC prep method.[53] Double crossover events were confirmed via PCR using GoTaq Green Master Mix (Promega, M7122).

Quantitative PCR. *K. rhaeticus* D1.1_mScarlet cultures were pelleted and resuspended in lysis buffer (SDS 1%, Tris-HCL 50 mM, EDTA 10 mM, 0.1% Proteinase K (Thermo

https://doi.org/10.1021/acssynbio.1c00358
ACS Synth. Biol. 2021, 10, 3422−3434

Scientific, EO0491)). Cell suspensions were held at 50 °C for 1 h to lyse cells, and genome and plasmid DNA were purified using the phenol−chloroform method. Forward and reverse primer sets for the *K. rhaeticus* chromosome and pSeva plasmid were selected using Primer3 (doi:10.1093/bioinformatics/btm091). Chromosome and pSeva plasmid abundance were measured using the Luna Universal qPCR Master Mix (NEB, M3003) on the MasterCycler ep Realplex Real-time PCR system (Eppendorf). Relative copies of pSeva plasmid to Chromosome were calculated from CT values using the Pfaffl method.[54]

AHL Induction Assays. For protein expression assays both *E. coli* and *K. rhaeticus* cultures were grown shaking to mid exponential phase. Cells treated with 50 nM (*E. coli*) or 50 μM (*K. rhaeticus*) of AHL (*N*-Acyl homoserine lactone, Sigma Aldrich K3255) and induced for approximately 4 doubling times (i.e., 2 or 16 h respectively). Cells were harvested and corrected for by OD_{600} before further analysis was performed.

Chromoprotein Expression. *K. rhaeticus* starter cultures were grown in HS-glucose media with chloramphenicol antibiotic at 35 μg/mL for 3 days prior to inoculation of 5 mL of HS-glucose in 24-well deep well plates. The plate was grown static for 5 days at 30 °C to grow pellicles. Pellicles were then removed, washed in sterile PBS for 10 min and imaged. Cell pellets were obtained by digestion of pellicles with 2% sterile cellulase in PBS (37 °C, 250 rpm for 8 h) before centrifugation at 13 000 rpm and removal of supernatant. Drying of pellicles was done by placing fresh pellicles on open Petri dishes and incubating at either 30 °C (16 h) or 60 °C (3 h) or by compressing the pellicle and leaving it a room temperature (24 h).

SDS-PAGE and Western Blot. Amyloid associated samples intended for SDS-PAGE analysis were prepared as described previously.[55] Briefly, cell pellets were resuspended in 100 μL dH_2O and lyophilized. Amyloid containing samples to be monomerized were treated with formic Acid, frozen and lyophilized a second time. All samples were resuspended in 8 M urea and loading buffer (2% SDS, 0.2 M Tris-HCl pH 6.8, 0.01% bromophenol blue, 10% glycerol, 2 mM DTT) before being heated at 95 °C and separated on in 12% SDS-PAGE gels. Proteins were transferred by semidry Western Blot onto PVDF membranes visualized with polyclonal antibody and BCIP/NBT (Promega, S3771).

Nonamyloidal samples were treated with protease inhibitor (Roche complete) before fractions separated and harvested. Cell fractions were resuspended in loading buffer and heated at 95 °C for 10 min. Supernatant fractions were TCA precipitated, washed with acetone, resuspended in loading buffer, and heated at 95 °C. Proteins samples were separated on 12−15% SDS-PAGE gels. Gels were stained with SimplyBlue SafeStain (ThermoFisher Scientific) and when required, transferred by semidry Western Blot onto PVDF membranes visualized with polyclonal antibody and BCIP/NBT (Promega, S3771). Antibodies used in this study included a monoclonal α-his-antibody (BioLegend, 652502) and polyclonal α-CsgA-antibody and α-TasA-antibody.

Transmission Electron Microscopy (TEM). *E. coli* and *K. rhaeticus* cultures were prepared with 100 nM AHL but further prepared as described above. Sample Pellets were resuspended in 300 μL HEPES buffer (pH 7.5). For *K. rhaeticus* samples were further treated with 20% cellulase for 4 h at 37 °C, before centrifuged again to wash away excess cellulose and resuspended in 300 μL HEPES buffer (pH 7.5). Two μL samples were spotted onto freshly glow discharged Formvar/Carbon on 300 Mesh Nickel grids (Agar Scientific) and blocked for 10 min with BHN1 (1% BSA, 50 mM HEPES, 150 mM NaCl, pH 7.5). Grids were then incubated for 30 min with polyclonal α-CsgA-antibody (1:10 in BHN1, washed twice with BHN2 (0.1% BSA, 50 mM HEPES, 150 mM NaCl, pH 7.5), incubated with secondary anti-Rabbit IgG-Gold coupled antibody (1/10 in BHN1) (Anti-Mouse IgG (whole molecule)−Gold antibody produced in goat (Sigma, G7652), washed twice in BHN2 and HN (50 mM HEPES, 150 mM NaCl, pH 7.5) before being stained with uranyl acetate. The FEI Tecnai G2 Spirit TWIN was used to visualize the cells on the grid.

Material Strength Tests. Pellicles were dried flat using a heated press set to 120 °C and 1 ton of pressure. Dog bone test specimens were cut out of the dried cellulose and specimen ends reinforced with card. Dots were marked on the surface of each specimen for the optical measurement of displacement. Tensile tests were conducted with a Deben Microtest Tensile Stage. Seven samples were measured per material, with results normalized for sample thickness.

Beta-Lactamase Nitrocefin Assay. Beta-lactamase activity was measured using Nitrocefin (Stratech, B6052) as per the manufacturer's instructions. Samples were induced as described above, and the extracellular supernatant fraction was removed post centrifugation. Extracellular fractions were equilibrated and diluted in 10× PBS (pH 7.5) at either 1:100 or 1:10 for *E. coli* or *K. rhaeticus*, respectively. Beta-lactamase converts nitrocefin from a yellow to a red substrate, and the enzyme activity was calculated as the rate of change of absorbance (490 nm, Synergy HT plate reader) over the linear region of a graph.

■ ASSOCIATED CONTENT

Supporting Information

The Supporting Information is available free of charge at https://pubs.acs.org/doi/10.1021/acssynbio.1c00358.

Supplementary Figure S1: Dehydration of chromoprotein pellicle samples; Supplementary Figure S2: Design of a CRISPR-regulator KTK plasmid; Supplementary Figure S3: Characterization of *K. rhaeticus* and *E. coli* heterologously expressing the whole *E. coli* Curli system; Supplementary Figure S4: Exploiting the T8SS using KTK to secrete heterologous cargo proteins in *E. coli*; Supplementary Figure S5: The dry pellicle weight of unengineered (WT) and engineered strains expressing the heterologous Curli system (D2.2_curli) and a Curli-based secretion system exporting ELP proteins (EFG-N22ELP); Supplementary Guide: KTK: a detailed introduction and guide (PDF)

Supplementary Tables S1−S3 (XLSX)

■ AUTHOR INFORMATION

Corresponding Author

Tom Ellis − *Imperial College Centre for Synthetic Biology and Department of Bioengineering, Imperial College London, London SW7 2AZ, U.K.;* orcid.org/0000-0001-5392-976X; Email: t.ellis@imperial.ac.uk

https://doi.org/10.1021/acssynbio.1c00358
ACS Synth. Biol. 2021, 10, 3422−3434

Authors

Vivianne J. Goosens − *Imperial College Centre for Synthetic Biology and Department of Bioengineering, Imperial College London, London SW7 2AZ, U.K.*

Kenneth T. Walker − *Imperial College Centre for Synthetic Biology and Department of Bioengineering, Imperial College London, London SW7 2AZ, U.K.*

Silvia M. Aragon − *Imperial College Centre for Synthetic Biology and Department of Life Sciences, Imperial College London, London SW7 2AZ, U.K.*

Amritpal Singh − *Imperial College Centre for Synthetic Biology and Department of Bioengineering, Imperial College London, London SW7 2AZ, U.K.*

Vivek R. Senthivel − *Imperial College Centre for Synthetic Biology and Department of Bioengineering, Imperial College London, London SW7 2AZ, U.K.*

Linda Dekker − *Imperial College Centre for Synthetic Biology and Department of Life Sciences, Imperial College London, London SW7 2AZ, U.K.*

Joaquin Caro-Astorga − *Imperial College Centre for Synthetic Biology and Department of Bioengineering, Imperial College London, London SW7 2AZ, U.K.*

Marianne L. A. Buat − *Department of Bioengineering, Imperial College London, London SW7 2AZ, U.K.*

Wenzhe Song − *Department of Aeronautics, Imperial College London, London SW7 2AZ, U.K.*

Koon-Yang Lee − *Department of Aeronautics, Imperial College London, London SW7 2AZ, U.K.*; orcid.org/0000-0003-0777-2292

Complete contact information is available at: https://pubs.acs.org/10.1021/acssynbio.1c00358

Author Contributions

VJG, KTW, VRS, and TE designed the research. VJG, KTW, SMA, AS, VRS, LD, JCA, MLAB, and WS performed the experiments. VJG, KTW, SMA, AS, WS, KYL, and TE analyzed the data. VJG and TE wrote the manuscript.

Funding

We acknowledge the following funders for supporting this work: the UK Engineering and Physical Sciences Research Council (EPSRC) for grants EP/N026489/1, EP/S032215/1 and studentship project 1846146, the UK Biotechnology and Biological Sciences Research Council (BBSRC) for training grant BB/R505808/1, the US Office of Naval Research Global (ONRG) and US Army CCDC DEVCOM for grant W911NF-18-1-0387, and the European CSA on biological standardization, BIOROBOOST (EU grant number 820699).

Notes

The authors declare no competing financial interest.

■ ACKNOWLEDGMENTS

We are grateful to A. Kan and N. Joshi for the synthetic Curli template, and to the Chapman Lab and Stanley-Wall Lab for CsgA and TasA-antibodies, respectively. The Steve Matthews lab, in particular G. Wu, for assisting with Curli protocols and lyophilization. The Polizzi lab, in particular R. Aw, and both P. Simpson and T. Pape at ICL-EM centre. And finally, to Ellis lab members C. Gilbert and W. Shaw for early discussions on Golden Gate syntax and standards.

■ REFERENCES

(1) Gilbert, C.; Ellis, T. Biological Engineered Living Materials: Growing Functional Materials with Genetically Programmable Properties. *ACS Synth. Biol.* **2019**, *8* (1), 1−15.

(2) Tang, T.-C.; An, B.; Huang, Y.; Vasikaran, S.; Wang, Y.; Jiang, X.; Lu, T. K.; Zhong, C. Materials Design by Synthetic Biology. *Nat. Rev. Mater.* **2021**, *6*, 332.

(3) Nguyen, P. Q.; Courchesne, N.-M. D.; Duraj-Thatte, A.; Praveschotinunt, P.; Joshi, N. S. Engineered Living Materials: Prospects and Challenges for Using Biological Systems to Direct the Assembly of Smart Materials. *Adv. Mater.* **2018**, *30* (19), 1704847.

(4) Lee, K. Y.; Buldum, G.; Mantalaris, A.; Bismarck, A. More than Meets the Eye in Bacterial Cellulose: Biosynthesis, Bioprocessing, and Applications in Advanced Fiber Composites. *Macromol. Biosci.* **2014**, *14* (1), 10−32.

(5) Jang, W. D.; Hwang, J. H.; Kim, H. U.; Ryu, J. Y.; Lee, S. Y. Bacterial Cellulose as an Example Product for Sustainable Production and Consumption. *Microb. Biotechnol.* **2017**, *10* (5), 1181−1185.

(6) Gwon, H.; Park, K.; Chung, S.-C.; Kim, R.-H.; Kang, J. K.; Ji, S. M.; Kim, N.-J.; Lee, S.; Ku, J.-H.; Do, E. C.; Park, S.; Kim, M.; Shim, W. Y.; Rhee, H. S.; Kim, J.-Y.; Kim, J.; Kim, T. Y.; Yamaguchi, Y.; Iwamuro, R.; Saito, S.; Kim, G.; Jung, I.-S.; Park, H.; Lee, C.; Lee, S.; Jeon, W. S.; Jang, W. D.; Kim, H. U.; Lee, S. Y.; Im, D.; Doo, S.-G.; Lee, S. Y.; Lee, H. C.; Park, J. H. A Safe and Sustainable Bacterial Cellulose Nanofiber Separator for Lithium Rechargeable Batteries. *Proc. Natl. Acad. Sci. U. S. A.* **2019**, *116*, 19288.

(7) Florea, M.; Hagemann, H.; Santosa, G.; Abbott, J.; Micklem, C. N.; Spencer-Milnes, X.; de Arroyo Garcia, L.; Paschou, D.; Lazenbatt, C.; Kong, D.; Chughtai, H.; Jensen, K.; Freemont, P. S.; Kitney, R.; Reeve, B.; Ellis, T. Engineering Control of Bacterial Cellulose Production Using a Genetic Toolkit and a New Cellulose-Producing Strain. *Proc. Natl. Acad. Sci. U. S. A.* **2016**, *113* (24), E3431−40.

(8) Walker, K. T.; Goosens, V. J.; Das, A.; Graham, A. E.; Ellis, T. Engineered Cell-to-Cell Signalling within Growing Bacterial Cellulose Pellicles. *Microb. Biotechnol.* **2019**, *12*, 611.

(9) Teh, M. Y.; Ooi, K. H.; Danny Teo, S. X.; Bin Mansoor, M. E.; Shaun Lim, W. Z.; Tan, M. H. An Expanded Synthetic Biology Toolkit for Gene Expression Control in Acetobacteraceae. *ACS Synth. Biol.* **2019**, *8* (4), 708−723.

(10) Singh, A.; Walker, K. T.; Ledesma-Amaro, R.; Ellis, T. Engineering Bacterial Cellulose by Synthetic Biology. *Int. J. Mol. Sci.* **2020**, *21* (23), 9185.

(11) Moore, S. J.; Lai, H.-E.; Kelwick, R. J. R.; Chee, S. M.; Bell, D. J.; Polizzi, K. M.; Freemont, P. S. EcoFlex: A Multifunctional MoClo Kit for E. Coli Synthetic Biology. *ACS Synth. Biol.* **2016**, *5* (10), 1059−1069.

(12) Engler, C.; Youles, M.; Gruetzner, R.; Ehnert, T.-M.; Werner, S.; Jones, J. D. G.; Patron, N. J.; Marillonnet, S. A Golden Gate Modular Cloning Toolbox for Plants. *ACS Synth. Biol.* **2014**, *3* (11), 839−843.

(13) Weber, E.; Engler, C.; Gruetzner, R.; Werner, S.; Marillonnet, S. A Modular Cloning System for Standardized Assembly of Multigene Constructs. *PLoS One* **2011**, *6* (2), e16765.

(14) Andreou, A. I.; Nakayama, N. Mobius Assembly: A Versatile Golden-Gate Framework towards Universal DNA Assembly. *PLoS One* **2018**, *13* (1), e0189892.

(15) Iverson, S. V.; Haddock, T. L.; Beal, J.; Densmore, D. M. CIDAR MoClo: Improved MoClo Assembly Standard and New E. Coli Part Library Enable Rapid Combinatorial Design for Synthetic and Traditional Biology. *ACS Synth. Biol.* **2016**, *5* (1), 99−103.

(16) Lee, M. E.; DeLoache, W. C.; Cervantes, B.; Dueber, J. E. A Highly Characterized Yeast Toolkit for Modular, Multipart Assembly. *ACS Synth. Biol.* **2015**, *4* (9), 975−986.

(17) Hernanz-Koers, M.; Gandía, M.; Garrigues, S.; Manzanares, P.; Yenush, L.; Orzaez, D.; Marcos, J. F. FungalBraid: A GoldenBraid-Based Modular Cloning Platform for the Assembly and Exchange of DNA Elements Tailored to Fungal Synthetic Biology. *Fungal Genet. Biol.* **2018**, *116*, 51−61.

(18) Wicke, N.; Radford, D.; Verrone, V.; Wipat, A.; French, C. E. BacilloFlex: A Modular DNA Assembly Toolkit for *Bacillus subtilis*. *bioRxiv*, September 6, 2017. DOI: 10.1101/185108.
(19) Martella, A.; Matjusaitis, M.; Auxillos, J.; Pollard, S. M.; Cai, Y. EMMA: An Extensible Mammalian Modular Assembly Toolkit for the Rapid Design and Production of Diverse Expression Vectors. *ACS Synth. Biol.* **2017**, *6* (7), 1380−1392.
(20) Vasudevan, R.; Gale, G. A. R.; Schiavon, A. A.; Puzorjov, A.; Malin, J.; Gillespie, M. D.; Vavitsas, K.; Zulkower, V.; Wang, B.; Howe, C. J.; Lea-Smith, D. J.; McCormick, A. J. CyanoGate: A Modular Cloning Suite for Engineering Cyanobacteria Based on the Plant MoClo Syntax. *Plant Physiol.* **2019**, *180* (1), 39.
(21) Chiasson, D.; Giménez-Oya, V.; Bircheneder, M.; Bachmaier, S.; Studtrucker, T.; Ryan, J.; Sollweck, K.; Leonhardt, H.; Boshart, M.; Dietrich, P.; Parniske, M. A Unified Multi-Kingdom Golden Gate Cloning Platform. *Sci. Rep.* **2019**, *9* (1), 10131.
(22) Wu, D.; Schandry, N.; Lahaye, T. A Modular Toolbox for Golden-Gate-Based Plasmid Assembly Streamlines the Generation of *Ralstonia Solanacearum* Species Complex Knockout Strains and Multi-Cassette Complementation Constructs: A Golden-Gate Toolkit for the *Rssc*. *Mol. Plant Pathol.* **2018**, *19* (6), 1511−1522.
(23) Valenzuela-Ortega, M.; French, C. Joint Universal Modular Plasmids (JUMP): A Flexible and Comprehensive Platform for Synthetic Biology. *bioRxiv*, October 10, 2019. DOI: 10.1101/799585.
(24) Geddes, B. A.; Mendoza-Suárez, M. A.; Poole, P. S. A Bacterial Expression Vector Archive (BEVA) for Flexible Modular Assembly of Golden Gate-Compatible Vectors. *Front. Microbiol.* **2019**, *9*, 3345.
(25) Evans, M. L.; Chapman, M. R. Curli Biogenesis: Order out of Disorder. *Biochim. Biophys. Acta, Mol. Cell Res.* **2014**, *1843* (8), 1551−1558.
(26) Chen, A. Y.; Deng, Z.; Billings, A. N.; Seker, U. O. S.; Lu, M. Y.; Citorik, R. J.; Zakeri, B.; Lu, T. K. Synthesis and Patterning of Tunable Multiscale Materials with Engineered Cells. *Nat. Mater.* **2014**, *13* (5), 515−523.
(27) Seker, U. O. S.; Chen, A. Y.; Citorik, R. J.; Lu, T. K. Synthetic Biogenesis of Bacterial Amyloid Nanomaterials with Tunable Inorganic-Organic Interfaces and Electrical Conductivity. *ACS Synth. Biol.* **2017**, *6* (2), 266−275.
(28) Birnbaum, D. P.; Manjula-Basavanna, A.; Kan, A.; Joshi, N. S. Hybrid Living Capsules Autonomously Produced by Engineered Bacteria. *bioRxiv*, November 24, 2020. DOI: 10.1101/2020.11.23.394965.
(29) Nguyen, P. Q.; Botyanszki, Z.; Tay, P. K. R.; Joshi, N. S. Programmable Biofilm-Based Materials from Engineered Curli Nanofibres. *Nat. Commun.* **2014**, *5*, 4945.
(30) Florea, M.; Reeve, B.; Abbott, J.; Freemont, P. S.; Ellis, T. Genome Sequence and Plasmid Transformation of the Model High-Yield Bacterial Cellulose Producer Gluconacetobacter Hansenii ATCC 53582. *Sci. Rep.* **2016**, *6*, 23635.
(31) Durante-Rodríguez, G.; de Lorenzo, V.; Martínez-García, E. The Standard European Vector Architecture (SEVA) Plasmid Toolkit. In *Pseudomonas Methods and Protocols*; Filloux, A., Ramos, J.-L., Eds.; Springer New York: New York, NY, 2014; pp 469−478. DOI: 10.1007/978-1-4939-0473-0_36.
(32) Liu, L.-P.; Yang, X.; Zhao, X.-J.; Zhang, K.-Y.; Li, W.-C.; Xie, Y.-Y.; Jia, S.-R.; Zhong, C. A Lambda Red and FLP/FRT-Mediated Site-Specific Recombination System in *Komagataeibacter Xylinus* and Its Application to Enhance the Productivity of Bacterial Cellulose. *ACS Synth. Biol.* **2020**, *9* (11), 3171−3180.
(33) Liljeruhm, J.; Funk, S. K.; Tietscher, S.; Edlund, A. D.; Jamal, S.; Wistrand-Yuen, P.; Dyrhage, K.; Gynnå, A.; Ivermark, K.; Lövgren, J.; Törnblom, V.; Virtanen, A.; Lundin, E. R.; Wistrand-Yuen, E.; Forster, A. C. Engineering a Palette of Eukaryotic Chromoproteins for Bacterial Synthetic Biology. *J. Biol. Eng.* **2018**, *12* (1), 8.
(34) Van Gerven, N.; Klein, R. D.; Hultgren, S. J.; Remaut, H. Bacterial Amyloid Formation: Structural Insights into Curli Biogensis. *Trends Microbiol.* **2015**, *23* (11), 693−706.
(35) Kan, A.; Birnbaum, D. P.; Praveschotinunt, P.; Joshi, N. S. Congo Red Fluorescence for Rapid *In Situ* Characterization of Synthetic Curli Systems. *Appl. Environ. Microbiol.* **2019**, *85* (13), e00434−19.
(36) Botyanszki, Z.; Tay, P. K. R.; Nguyen, P. Q.; Nussbaumer, M. G.; Joshi, N. S. Engineered Catalytic Biofilms: Site-Specific Enzyme Immobilization onto E. Coli Curli Nanofibers. *Biotechnol. Bioeng.* **2015**, *112* (10), 2016−2024.
(37) Van Gerven, N.; Goyal, P.; Vandenbussche, G.; De Kerpel, M.; Jonckheere, W.; De Greve, H.; Remaut, H. Secretion and Functional Display of Fusion Proteins through the Curli Biogenesis Pathway. *Mol. Microbiol.* **2014**, *91* (5), 1022−1035.
(38) Sivanathan, V.; Hochschild, A. Generating Extracellular Amyloid Aggregates Using E. Coli Cells. *Genes Dev.* **2012**, *26* (23), 2659−2667.
(39) Wang, M.; Huang, M.; Zhang, J.; Ma, Y.; Li, S.; Wang, J. A Novel Secretion and Online-Cleavage Strategy for Production of Cecropin A in Escherichia Coli. *Sci. Rep.* **2017**, *7* (1), 7368.
(40) Tay, P. K. R.; Nguyen, P. Q.; Joshi, N. S. A Synthetic Circuit for Mercury Bioremediation Using Self-Assembling Functional Amyloids. *ACS Synth. Biol.* **2017**, *6* (10), 1841−1850.
(41) Zhong, C.; Gurry, T.; Cheng, A. A.; Downey, J.; Deng, Z.; Stultz, C. M.; Lu, T. K. Strong Underwater Adhesives Made by Self-Assembling Multi-Protein Nanofibres. *Nat. Nanotechnol.* **2014**, *9* (10), 858−866.
(42) Nussbaumer, M. G.; Nguyen, P. Q.; Tay, P. K. R.; Naydich, A.; Hysi, E.; Botyanszki, Z.; Joshi, N. S. Bootstrapped Biocatalysis: Biofilm-Derived Materials as Reversibly Functionalizable Multi-enzyme Surfaces. *ChemCatChem* **2017**, *9* (23), 4328−4333.
(43) Salis, H. M.; Mirsky, E. A.; Voigt, C. A. Automated Design of Synthetic Ribosome Binding Sites to Control Protein Expression. *Nat. Biotechnol.* **2009**, *27* (10), 946−950.
(44) Borkowski, O.; Ceroni, F.; Stan, G.-B.; Ellis, T. Overloaded and Stressed: Whole-Cell Considerations for Bacterial Synthetic Biology. *Curr. Opin. Microbiol.* **2016**, *33*, 123−130.
(45) Costa, T. R.; Felisberto-Rodrigues, C.; Meir, A.; Prevost, M. S.; Redzej, A.; Trokter, M.; Waksman, G. Secretion Systems in Gram-Negative Bacteria: Structural and Mechanistic Insights. *Nat. Rev. Microbiol.* **2015**, *13* (6), 343−359.
(46) Hospenthal, M. K.; Costa, T. R. D.; Waksman, G. A Comprehensive Guide to Pilus Biogenesis in Gram-Negative Bacteria. *Nat. Rev. Microbiol.* **2017**, *15* (6), 365−379.
(47) Roberts, S.; Dzuricky, M.; Chilkoti, A. Elastin-like Polypeptides as Models of Intrinsically Disordered Proteins. *FEBS Lett.* **2015**, *589* (19), 2477−2486.
(48) Gilbert, C.; Tang, T.-C.; Ott, W.; Dorr, B. A.; Shaw, W. M.; Sun, G. L.; Lu, T. K.; Ellis, T. Living Materials with Programmable Functionalities Grown from Engineered Microbial Co-Cultures. *Nat. Mater.* **2021**, *20*, 691.
(49) Erskine, E.; MacPhee, C. E.; Stanley-Wall, N. R. Functional Amyloid and Other Protein Fibers in the Biofilm Matrix. *J. Mol. Biol.* **2018**, *430* (20), 3642−3656.
(50) Bongers, R. S.; Veening, J.-W.; Van Wieringen, M.; Kuipers, O. P.; Kleerebezem, M. Development and Characterization of a Subtilin-Regulated Expression System in Bacillus Subtilis: Strict Control of Gene Expression by Addition of Subtilin. *Appl. Environ. Microbiol.* **2005**, *71* (12), 8818−8824.
(51) Mierau, I.; Olieman, K.; Mond, J.; Smid, E. J. Optimization of the Lactococcus Lactis Nisin-Controlled Gene Expression System NICE for Industrial Applications. *Microb. Cell Fact.* **2005**, *4* (1), 16.
(52) Tabor, S. Expression Using the T7 RNA Polymerase/Promoter System. *Curr. Protoc. Mol. Biol.* **1990**, DOI: 10.1002/0471142727.mb1602s11.
(53) Blount, B. A.; Driessen, M. R. M.; Ellis, T. GC Preps: Fast and Easy Extraction of Stable Yeast Genomic DNA. *Sci. Rep.* **2016**, *6* (1), 26863.
(54) Pfaffl, M. W. A New Mathematical Model for Relative Quantification in Real-Time RT-PCR. *Nucleic Acids Res.* **2001**, *29* (9), 45e−445.
(55) Rouse, S. L.; Hawthorne, W. J.; Berry, J. L.; Chorev, D. S.; Ionescu, S. A.; Lambert, S.; Stylianou, F.; Ewert, W.; Mackie, U.;

Morgan, R. M. L.; Otzen, D.; Herbst, F. A.; Nielsen, P. H.; Dueholm, M.; Bayley, H.; Robinson, C. V.; Hare, S.; Matthews, S. A New Class of Hybrid Secretion System Is Employed in Pseudomonas Amyloid Biogenesis. *Nat. Commun.* **2017**, *8* (1), 263.

https://doi.org/10.1021/acssynbio.1c00358
ACS Synth. Biol. 2021, 10, 3422−3434